Supporting Information

Enabling rare-earth samarium into $MnIn_2S_4$ micron flowers for visible-light-driven H_2O_2 generation and organic pollutant degradation

Zhichao Yi,[a] Jianhong Wu, [a] Chensheng Zhou,[a] Zhiquan Lai, [a] Kailian Zhang,[a] Kangqiang Lu,[a] Weiya Huang,[a] Changlin Yu,[b] Kai Yang[a]*

a. School of Chemistry and Chemical Engineering, Jiangxi Provincial Key Laboratory of Functional Crystalline Materials Chemistry, Jiangxi University of Science and Technology, Ganzhou 341000, Jiangxi, China.

b. School of Chemical Engineering, Guangdong University of Petrochemical Technology, Maoming 525000, Guangdong, China.

*Corresponding author: Kai Yang, Ph. D. Professor, E-mail: yangkai@jxust.edu.cn

Experimental Section

SI.1 Material preparation

Synthesis of $MnIn_2S_4$ powder: 0.405 g of $MnCl_2$, 1.06 g of $InCl_3 \cdot 4\ H_2O$, and 0.75 g of CH_3CSNH_2 were weighed and added to a 60 mL mixed solution of deionized water and anhydrous ethanol (volume ratio = 1:1). The mixture was stirred with a magnetic stirrer until completely dissolved. The solution was then transferred to a 100 mL Teflon-lined autoclave, sealed, and placed in a forced-air oven for hydrothermal reaction at 180 ℃ for 12 h. After the reaction, the product was collected, washed multiple times with deionized water and anhydrous ethanol, rinsed thoroughly, and dried at 60 °C for 12 h.

The procedure for preparing Sm-doped $MnIn_2S_4$ was largely identical to that of the synthesis of $MnIn_2S_4$ described above, with the only difference being the addition of varying amounts of Sm $(NO_3)_3 \cdot 6\ H_2O$ (Sm/Mn molar ratio = 2%, 5%, 10%) to the mixed solution. This yielded Sm-doped $MnIn_2S_4$ powders with different loadings, denoted as $MnIn_2S_4$ n%Sm (n = 2, 5, 10). The preparation flowchart is shown in Figure S1.

SI.2 Characterizations

X-ray diffraction (XRD, Cu $K\alpha$, Bruker D8, λ = 0.15406 nm) was used to identify the crystal structures of the samples. The morphological features were examined by scanning electron microscopy (SEM, ZEISS Sigma 500) and high-resolution transmission electron microscopy (HRTEM, FEI-Technai-G20). Spherical Aberration Corrected Transmission Electron Microscope (AC–STEM) images were obtained using

STEM (Thermo Scientific spectra 300) with a spherical aberration corrector. Fourier transform infrared (FT-IR) spectra could be acquired by the FT-IR spectrometer (Nicolet 5700). The elemental chemical state and surface property were analyzed by X-ray photoelectron spectra (XPS, Nexsa, Al K Alpha). N_2 adsorption-desorption and CO_2 adsorption capacity tests were conducted on physical adsorption instrument (ASAP 2020). The optical absorption properties of the samples were studied using UV-vis diffuse reflectance spectra (DRS, Shimadzu UV-2600 instrument) with $BaSO_4$ as the basic reference. Hitachi F-4500 fluorescence spectrometer with an excitation wavelength of 365 nm could obtain photoluminescence (PL) spectra. Contact angle measurements were carried out using the static drop method using a Fangrui Instrument Company JCY contact angle meter. EPR spectrum was examined by an electron paramagnetic resonance spectrometer (Bruker ER200 SLC, Germany) at room temperature. Photoelectrochemical measurements including photocurrent-time response (I-T), electrochemical impedance spectroscopy (EIS), linear scanning voltammetry (LSV), mott-schottky (MS) and cyclic voltammetry (CV) were performed in a three-electrode cell (CHI-660E, Shanghai Chen Hua). The working electrode was from the catalyst being coated on the conductive glass. Ag/AgCl was as the reference electrode, Pt wire was as the counter electrode, and the electrolyte was 0.1 M Na_2SO_4 (pH = 7). The corresponding parameter information was as that amplitude was 5 mV/s, high frequency was 100 kHz, low frequency was 1 Hz, and potential was 0.23 V. The interval between light turns for photocurrent testing was 20 seconds.

SI.3 Photocatalytic reaction

The photocatalytic production of H_2O_2 was carried out in an open-type photocatalytic reaction vessel. 20 mg of catalyst was weighed and dispersed in 50 mL of a 10% ethanol aqueous solution. After ultrasonication for 5 minutes, circulating cooling water was turned on to maintain the entire reaction system at room temperature. At the same time, a magnetic stirrer was activated to ensure uniform mixing of the reaction solution and the catalyst. The mixture was then exposed to light from a 300-W xenon lamp (548.75 mW/cm^2) equipped with a filter with a wavelength cut-off of 420 nm for 1 hour. The reactive temperature was maintained at 25 ^{o}C by cooling cycle water. After that, 2 mL of the sample was taken using a dropper. The sample was subjected to centrifugation to separate the liquid from the catalyst; 500 μL of the upper clear liquid was then taken and mixed with 2 mL of potassium iodide solution and 50 μL of ammonium molybdate solution to allow for a complete reaction. The concentration of H_2O_2 in the solution was determined using a spectrophotometer.

The methylene blue solution prepared in the laboratory was used as a simulated pollutant for photocatalytic degradation. A 300 W xenon lamp ($\lambda \geqslant 420$ nm, 548.75 mW/cm^2) was used as a visible light source to degrade the tetracycline hydrochloride solution. The reactive temperature was maintained at 25 ^{o}C by cooling cycle water. The specific process is as follows: weighing 20 mg of the catalyst, dispersing it into 50 mL of 20 mg/L methylene blue solution, ultrasonicating for 5 minutes and performing a dark reaction for 30 minutes to saturate the adsorption of the catalyst. Then, it was irradiated for 2.5 hours, and taken the samples every half an hour. The concentration of methylene blue was measured with a liquid ultraviolet spectrophotometer, and the

degradation rate of pollutants was calculated based on the absorbance value.

Determination of free $\cdot O_2^-$ concentration: Nitroblue tetrazolium (NBT) could be reduced by O_2 to blue formazan, and 1 mol NBT can react with 4 mol of O_2. The concentration of generated $\cdot O_2^-$ was quantified by measuring the residual concentration of NBT on a UV-vis spectrophotometer.

Determination of free ·OH concentration: 7-hydroxycoumarin could react with ·OH by fluorescence formation. The concentration of generated ·OH was quantified by a fluorescence spectrum.

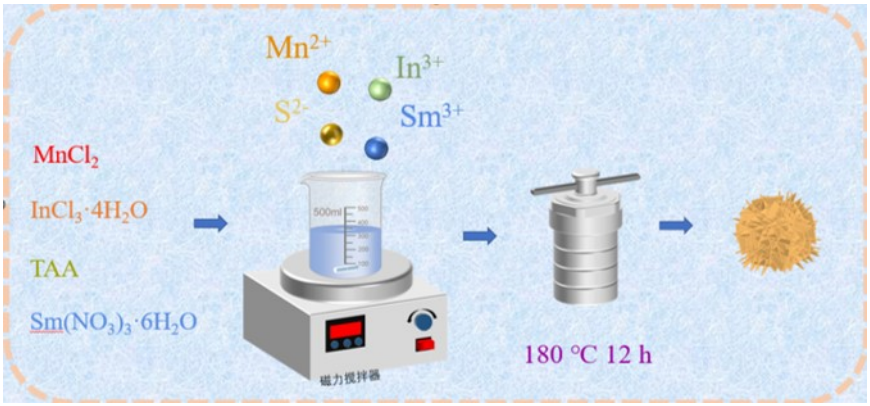

Fig. S1 Flowchart of hydrothermal synthesis of Sm-doped $MnIn_2S_4$.

.

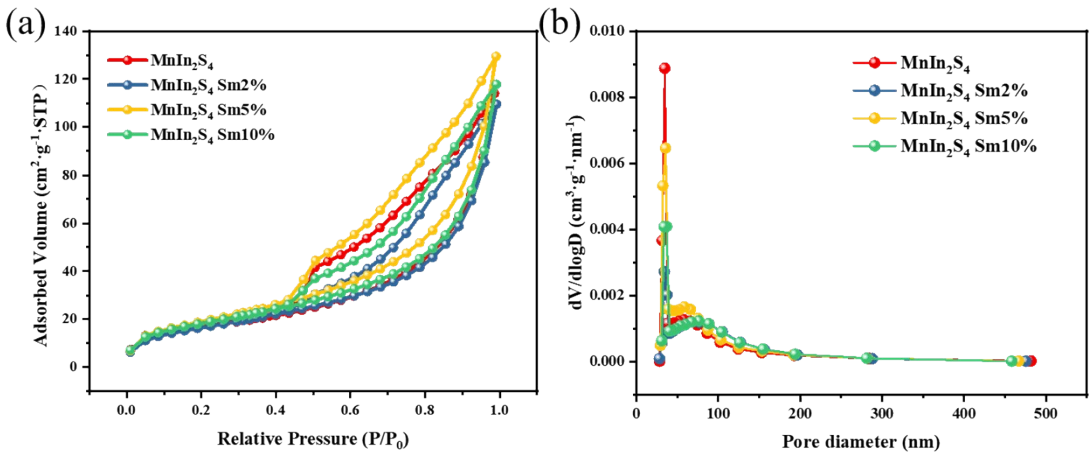

Fig. S2 (a) N_2 adsorption-desorption isotherm curves; (b) Pore size distribution diagrams.

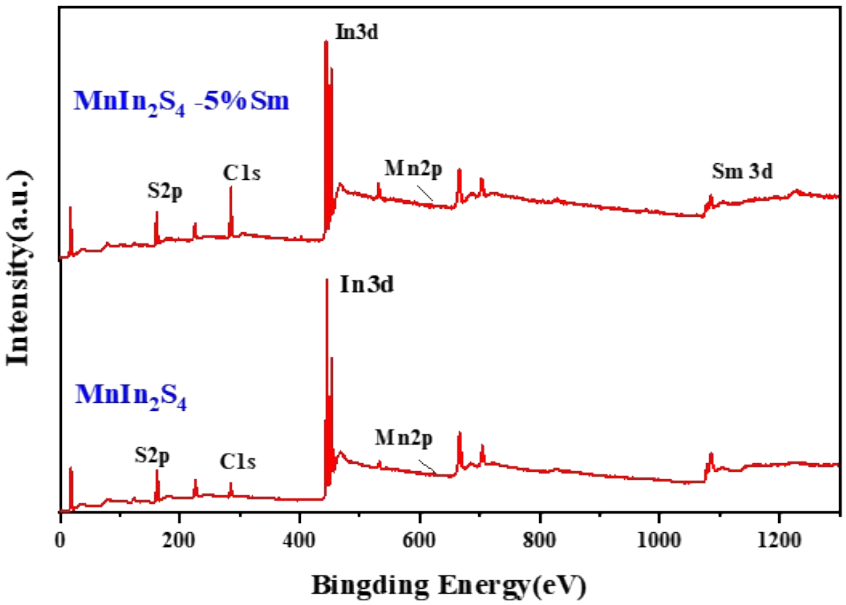

Fig. S3 XPS full spectrum.

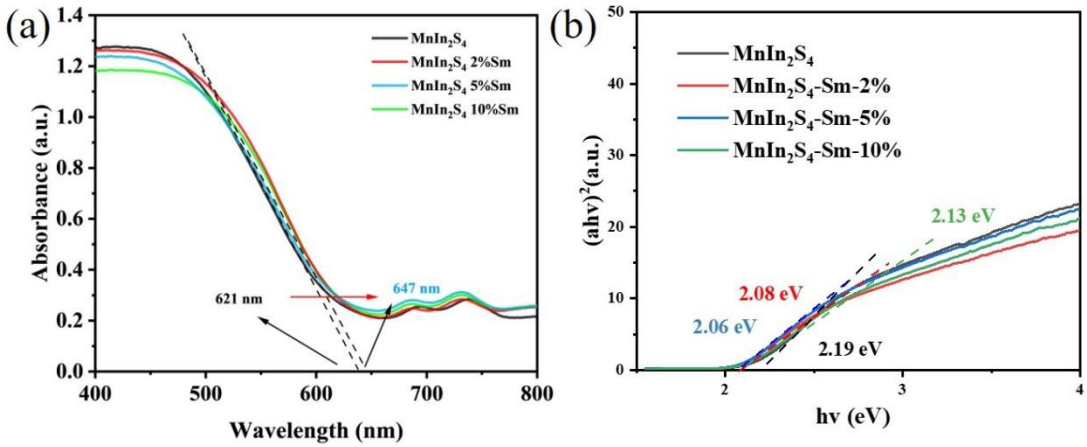

Fig. S4 (a) UV-Vis diffuse reflectance spectra; (b) $(\alpha hv)^2$-(hv) plots.

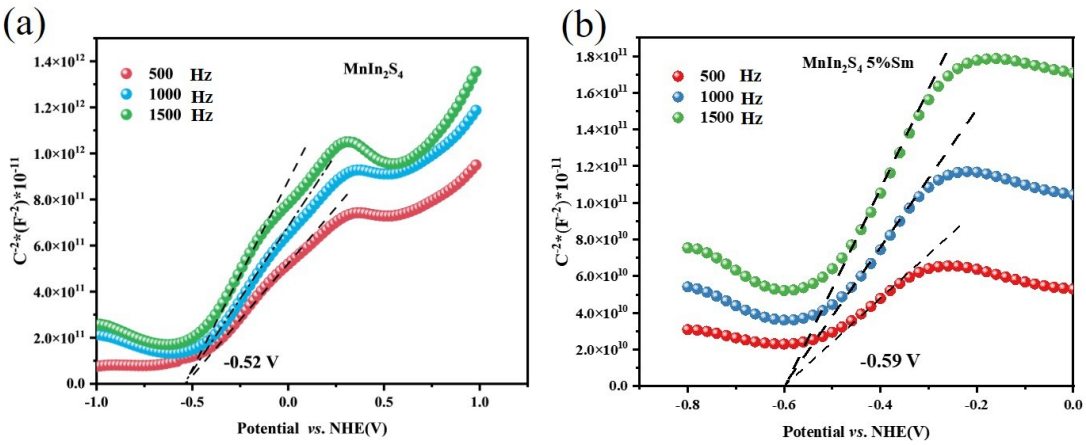

Fig. S5 Mott-Schottky plots of $MnIn_2S_4$ (a) and $MnIn_2S_4$-5%Sm (b), respectively.

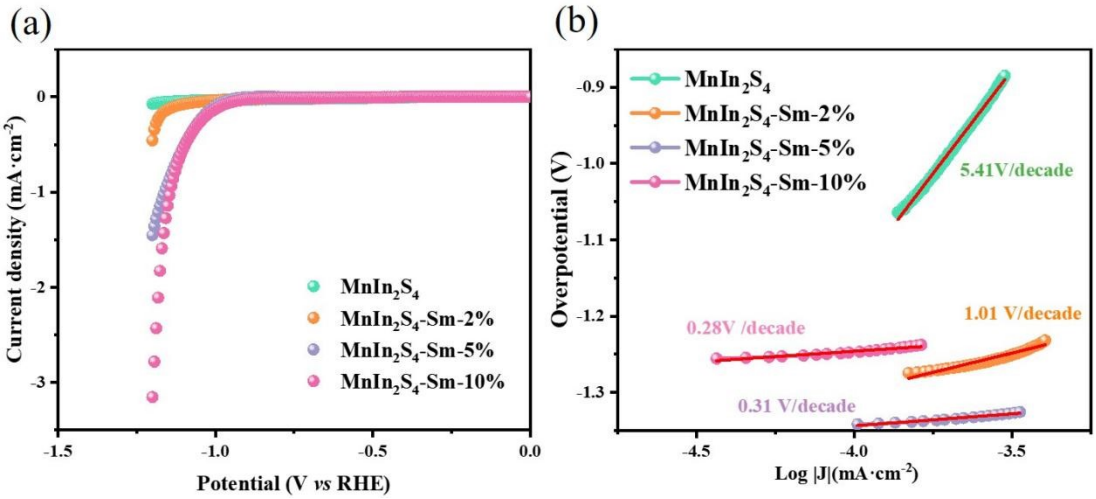

Fig. S6 (a) LSV diagrams; (b) Tafel slope diagrams.

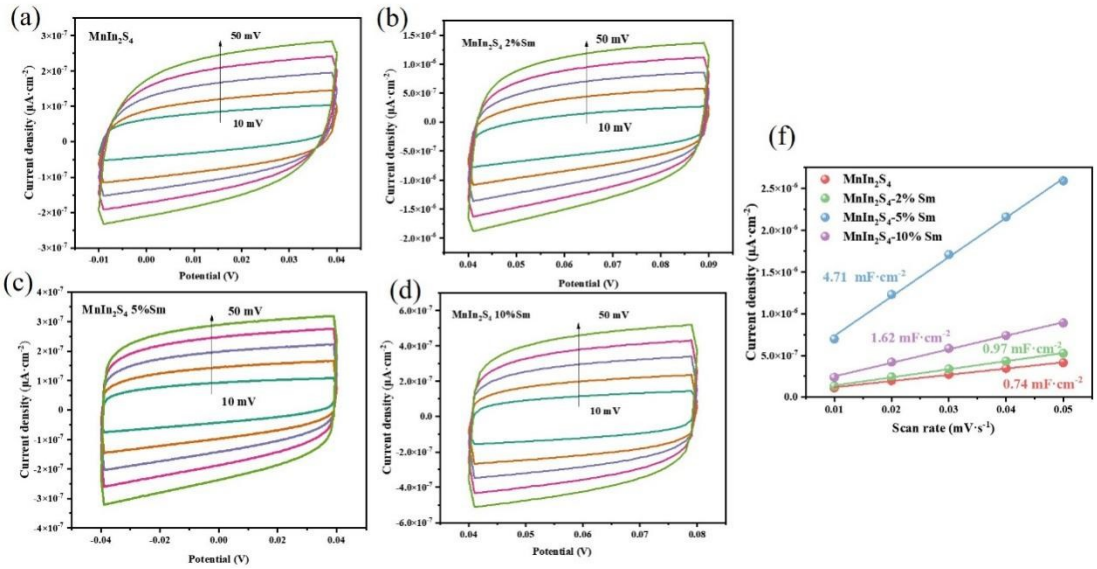

Fig. S7 (a-d) Cyclic voltammetry curves of samples; (e) Current density-scan rate plots of the samples.

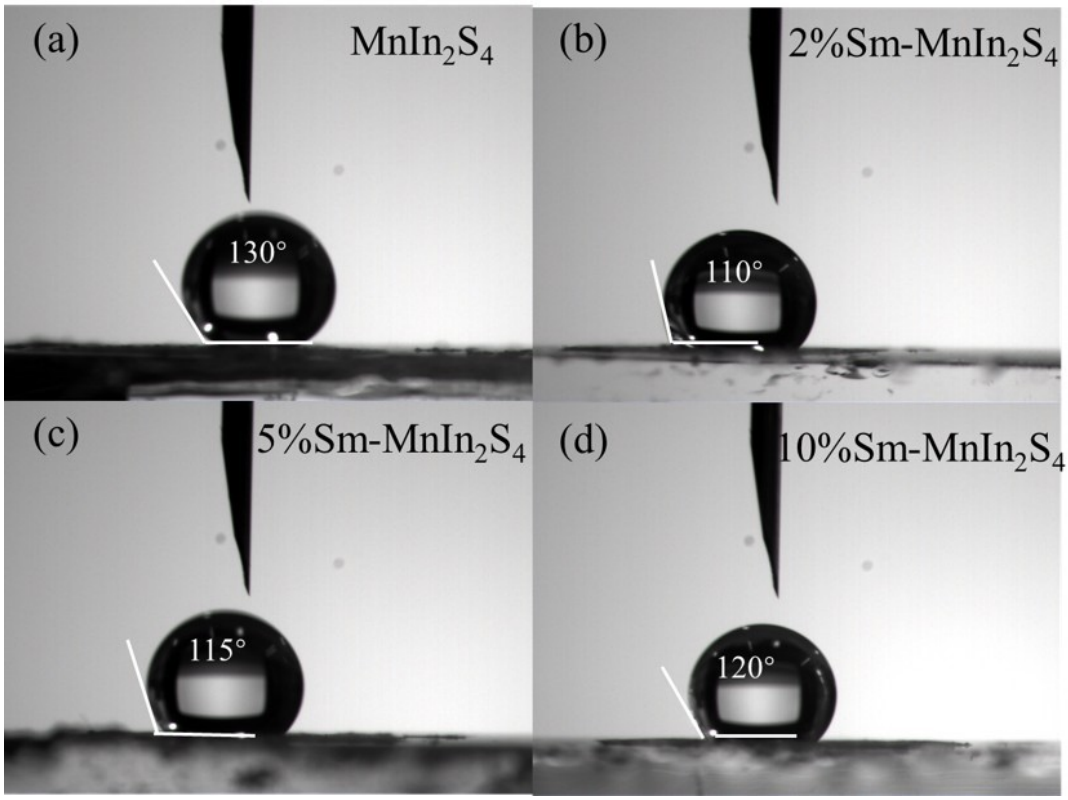

Fig. S8 Schematic diagrams of the contact angle between the sample surface and the reaction solution: (a) $MnIn_2S_4$; (b) $MnIn_2S_4$-2%Sm; (c) $MnIn_2S_4$-5%Sm; (d) $MnIn_2S_4$-10%Sm.

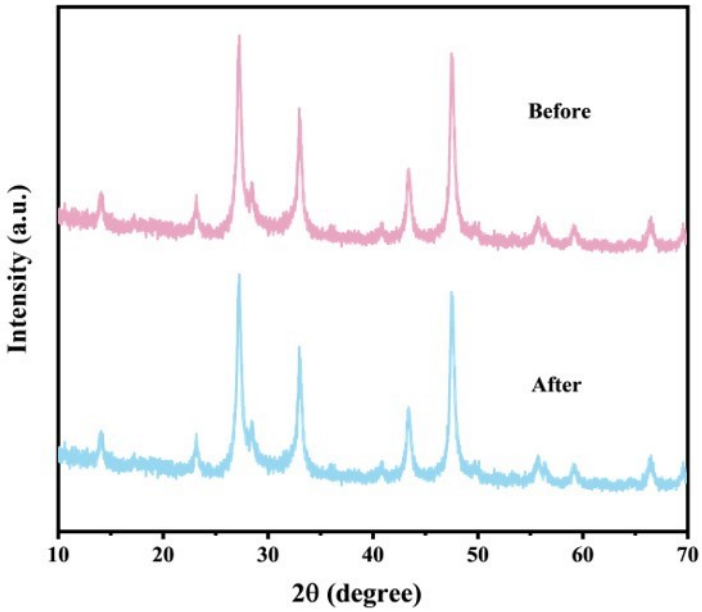

Fig. S9 XRD patterns before and after the reaction of $MnIn_2S_4$ 5%Sm.

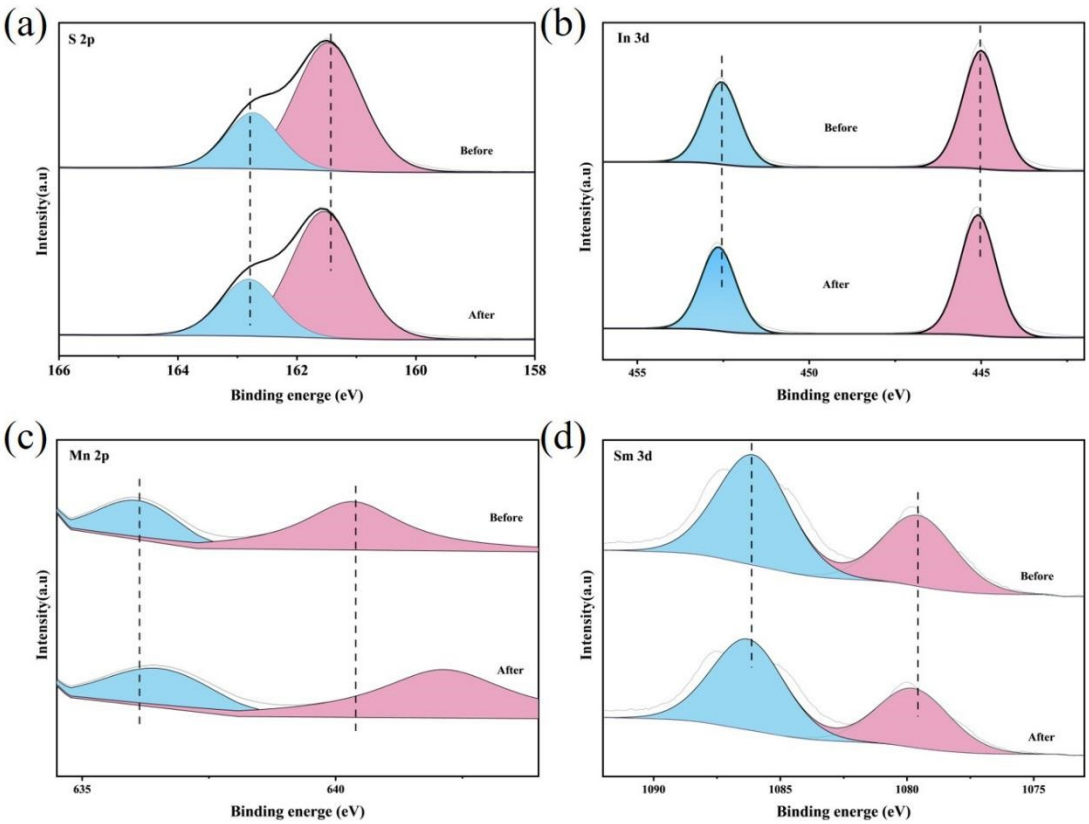

Fig. S10 XPS spectra before and after the reaction of $MnIn_2S_4$ 5%Sm.

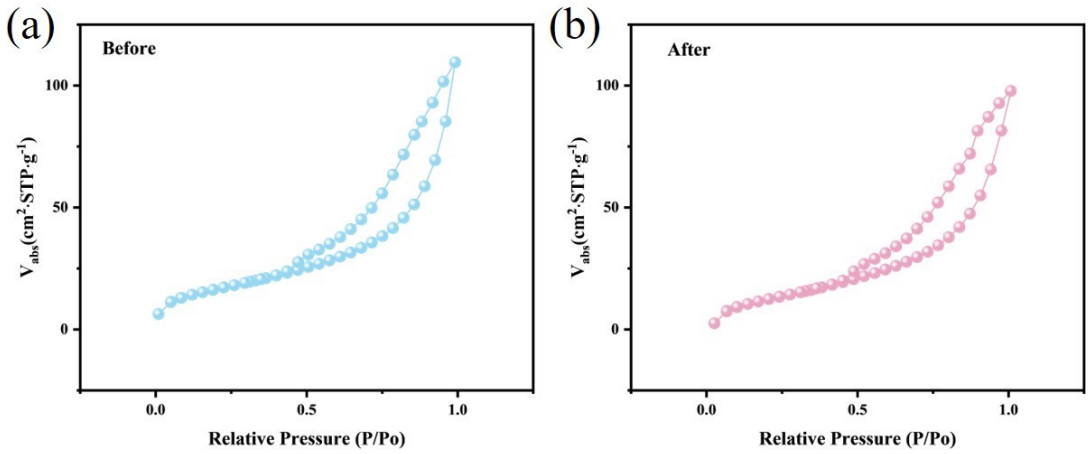

Fig. S11 BET patterns before and after the reaction of $MnIn_2S_4$ 5%Sm.

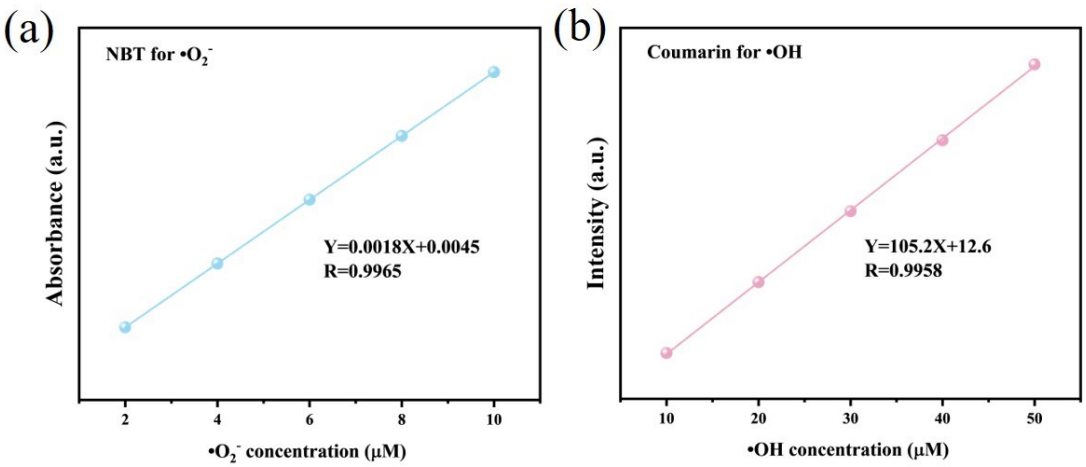

Fig. S12 (a) UV absorption spectra of superoxide radicals detected by NBT for $MnIn_2S_4$ 5%Sm under different light irradiation times; (b) Fluorescence spectra of hydroxyl radicals detected by coumarin for $MnIn_2S_4$ 5%Sm under different light irradiation times.

Table S1. Specific surface areas, pore volumes and average pore diameters of samples.

Sample	Specific surface area (m^2/g)	Pore volume (cm^3/g)	Average pore diameter (nm)
$MnIn_2S_4$	58.78	0.17	120.01
$MnIn_2S_4$-2%Sm	60.75	0.18	109.62
$MnIn_2S_4$-5%Sm	70.17	0.19	114.17
$MnIn_2S_4$-10%Sm	66.49	0.17	110.53

Table S2. Summary of equivalent circuit fitting parameters.

Samples	**Rs** **($\Omega \cdot cm^2$)**	**Rct** **($\Omega \cdot cm^2$)**	**CPE_{Y0}** **($S^n/\Omega \cdot cm^2$)**
$MnIn_2S_4$	51.82	5010	3.8×10^{-6}
$MnIn_2S_4$ 2%Sm	49.36	4900	3.5×10^{-6}
$MnIn_2S_4$ 5%Sm	41.69	1200	2.0×10^{-6}
$MnIn_2S_4$ 10%Sm	46.73	1800	1.8×10^{-6}

Table S3. Specific surface area, pore volume and average pore diameter of samples.

Sample	Specific surface area (m^2/g)	Pore volume (cm^3/g)	Average pore diameter (nm)
Pre-reaction $MnIn_2S_4$-5%Sm	70.17	0.19	114.17
Post-reaction $MnIn_2S_4$-5%Sm	68.68	0.18	112.46